Captopril Blunts Cardiac Remodeling, Prevents Dysfunction, and Improves Survival in Two Different Murine Models of Heart Failure

T. C-C. Hu[1], W. Bao[1], S. C. Lenhard[1], T. R. Schaeffer[1], T-L. Yue[1], B. M. Jucker[1], R. N. Willette[1]

[1]CVU-CEDD, GlaxoSmithKline, King of Prussia, PA, United States

Introduction Cardiac MRI is a reliable tool for monitoring the changes in cardiac morphology and function *in vivo* (1,2) and in heart failure (3,4). However, few studies have been performed to evaluate drug treatment in mouse cardiac hypertrophy models. With the advent of genetically engineered mice, murine models of pressure overload by transverse aortic constriction (TAC) and of myocardial infarction (MI) have been widely used to study the role of specific genes in the pathophysiology of cardiac hypertrophy and heart failure. It may be beneficial to use *in vivo* MRI techniques to accurately differentiate the severity of cardiac hypertrophy and myocardial function as well as to assess drug interactions in these murine MI models. Previous studies have demonstrated the dramatic benefit resulting from angiotensin-converting enzyme (ACE) inhibition in preventing cardiovascular disease (5). In the present study, we use *in vivo* cardiac MRI to assess the long-term effects of attenuating cardiac remodeling and improving cardiac function with Captopril (ACE inhibitor) in two different murine models of heart failure.

Methods Mice (CD1-ICR, 6-8 weeks) were anesthetized with intraperitoneal sodium pentobarbital and placed in a supine position. A midline cervical incision was made to intubate the trachea, and connected with a rodent ventilator. Mice were ventilated with a tidal volume of 0.2 ml and a respiratory rate of 105 breath per minute. The chest was opened by middle thoracotomy at upper sternum. Aortic banding was performed by ligating the transverse thoracic aorta between the innominate artery and left common carotid artery with a 27-gauge needle using a 7-0 silk suture. The needle was withdrawn after banding. The sham operated mice underwent similar thoracotomy without constricting the aorta. In the permanent myocardial infarction (MI) studies, permanent myocardial infarcts were produced by ligating the left anterior descending coronary artery (LAD). LAD was ligated at a position ~1 mm below left auricle with an 8-0 polypropylene monofilament suture. ECG was monitored during surgery. Captopril was given in drinking water (concentration: 1mg/ml).

During the non-invasive serial cardiac MRI experiments, the animals were induced and anaesthetized with a mixture of oxygen, and isoflurane (1-2%) anesthesia. The ECG signal was monitored and this signal was used to gate the MRI Fast Low Angle SHot (FLASH) sequence. All cardiac images were acquired on a 9.4 T Bruker BioSpec MRI spectrometer (Billerica, MA) using a standard volume coil.

Short-axis heart images were acquired using an ECG gated FLASH sequence. A pilot coronal image of the heart was obtained. This pilot coronal image provided a clear view of the heart apex. The short axis slices covered the entire left ventricle and part of the liver. A cine loop was generated for each slice with enough delays to cover the systole (ECG was triggered by R-wave, which is end-diastole). The imaging parameters were as follows: matrix dimensions, 128x128; TE, 2.3 ms; TR, 11.0 ms; slice thickness, 1 mm; FOV, 2.5 cm; 4 averages. All images were gated to be acquired directly after the ECG R-wave at end-diastole. Image analysis was performed using ANALYZE software package (AnalyzeDirect, KS), the ROI tools were used to select the areas of interest (septum and left ventricular free wall). Left-ventricular functional data was also analyzed providing left-ventricular end-diastolic volume (EDV), end-systolic volume (ESV), ejection fraction (EF), stroke volume (SV), cardiac output (CO), and LV mass data.

Results ECG gated cardiac MRI provided high quality images for left-ventricular function determination as shown in Figure 1 and Table 1. In addition, cardiac hypertrophy and heart failure can be induced by either aortic banding (AB) or myocardial infarction (MI) in mice. In the MI model of heart failure, Captopril improved both survival and EF compared with Vehicle group (60% vs 20% and 28% vs 22%, respectively (Figure 2 and Table 1). Similar observations were observed in the AB hypertropic model, which over time developed into heart failure. In both heart failure mouse models, disease progression was inhibited with Captopril.

Conclusions This study demonstrates that cardiac MRI can clearly track and monitor disease progression in two different murine heart failure models. The two different models have distinct heart failure progression timeframes (Figure 1). However, survival benefit and functional improvement could be demonstrated with Captopril in both models. In conclusion, cardiac MRI may be used to assess long-term effects of attenuating cardiac remodeling and improving cardiac function with pharmacological intervention.

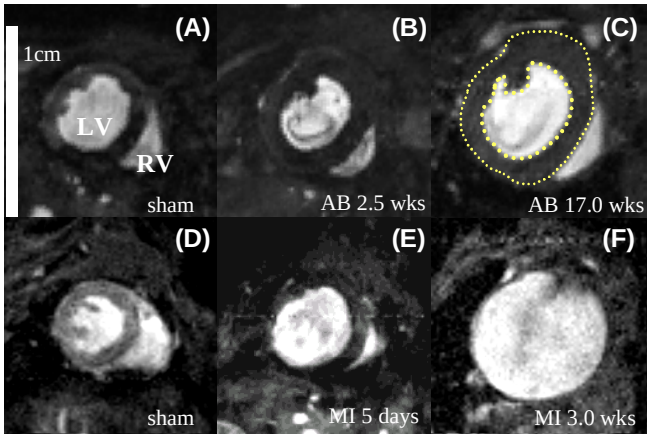

Figure 1. Examples of short-axis mouse heart images for (A),(B),(C) AB model and (D), (E), (F) MI model.

Figure 2. Survival curves for mouse (A) MI heart failure model (B) AB heart failure model. *P<0.05 Captopril vs Placebo (Vehicle) groups.

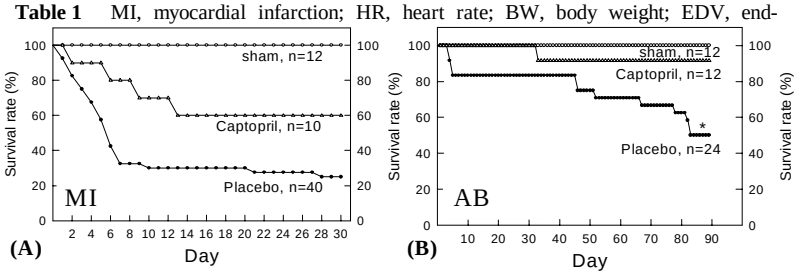

Table 1 MI, myocardial infarction; HR, heart rate; BW, body weight; EDV, end-diastolic volume; ESV, end-systolic volume; CO, cardiac output; LV Mass, left-ventricular mass; and EF, ejection fraction. Values are expressed as mean±SEM. $^{+}$P<0.01 t-test between the Sham and all other groups in MI. *P<0.05 t-test between Captopril and Vehicle groups in MI. ^P=0.17, t-test between Captopril and Vehicle groups in AB.

	MI (1.5 months post)			AB (4 months post)	
	Sham (n=7)	Vehicle (n=4)	Captopril (n=6)	Vehicle (n=7)	Captopril (n=11)
HR, bpm	319 ± 13	326 ± 24	336 ± 24	321 ± 16	358 ± 14
BW, g	36.5 ± 1.7	37.4 ± 1.1	39.8 ± 0.5	37.9 ± 1.3	39.0 ± 0.9
EDV, mm^3	93.5 ± 5.2+	280.7 ± 19.7	265.2 ± 20.2	93.0 ± 9.5	87.4 ± 4.2
ESV, mm^3	33.9 ± 4.2+	221.2 ± 21.7	191.8 ± 15.6	37.6 ± 6.5	34.9 ± 3.4
LV Mass, mg	132 ± 11	251 ± 9	243 ± 15	216 ± 15	188 ± 12^
CO, cm^3/min	18.9 ± 0.9	19.4 ± 2.1	24.3 ± 1.6	17.7 ± 1.7	18.7 ± 1.0
EF, %	**64.2 ± 3.1+**	**21.5 ± 2.4**	**27.8 ± 1.3***	60.7 ± 3.5	60.7 ± 2.7

Acknowledgment The authors thank C. Doe, and M.T. Li for stimulating discussions.

References

1. Zhou R, Pickup S, Glickson JD, Scott CH, Ferrari VA. Magn Reson Med 2003;49(4):760-764.
2. Wiesmann F, Frydrychowicz A, Rautenberg J, Illinger R, Rommel E, Haase A, Neubauer S. Am J Physiol Heart Circ Physiol 2002;283(3):H1065-71.
3. Nahrendorf M, Hiller KH, Hu K, Ertl G, Haase A, Bauer WR. Med Image Anal. 2003;7(3):369-75.
4. Yang Z, French BA, Gilson WD, Ross AJ, Oshinski JN, Berr SS. Circulation. 2001;103(15):E84.
5. Podesser BK, Schirnhofer J, Bernecker OY, Kroner A, Franz M, Semsroth S, Fellner B, Neumuller J, Hallstrom S, Wolner E. Circulation. 2002;106(12):I277-83.